Article

Cell Reports

Direct Conversion of Fibroblasts to Megakaryocyte Progenitors

Graphical Abstract

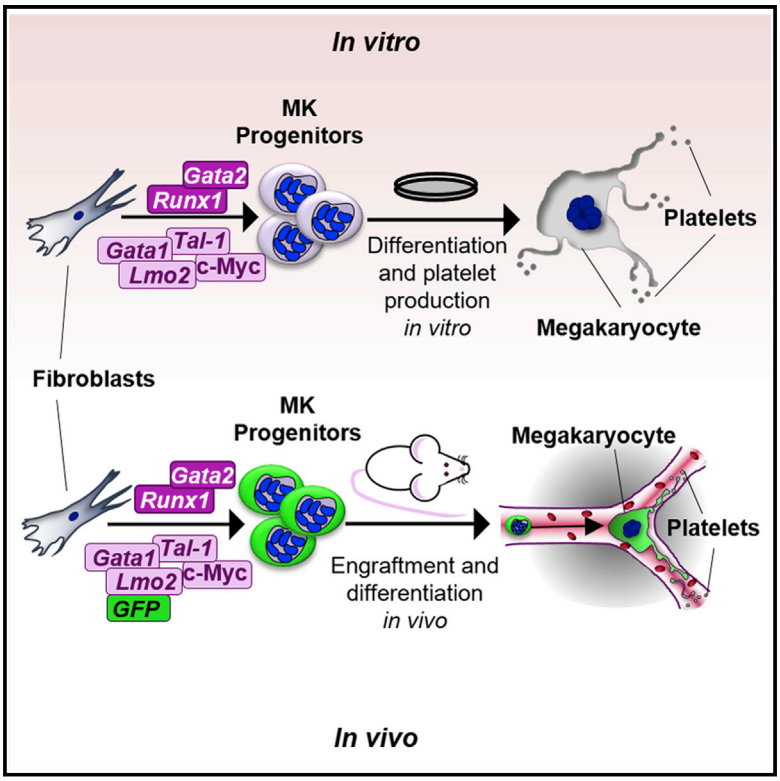

Highlights

- A defined set of six factors directly converts fibroblasts to megakaryocyte progenitors
- Transdifferentiated cells engraft and differentiate upon transplantation in NSG mice
- Megakaryocytes and platelets can be generated from fibroblasts of Fanconi anemia patients

Authors

Julian Pulecio, Oriol Alejo-Valle, Sandra Capellera-Garcia, ..., Juan A. Bueren, Johan Flygare, Angel Raya

Correspondence

jpulecio@cmrb.eu (J.P.), araya@cmrb.eu (A.R.)

In Brief

Pulecio et al. show that a cocktail of six transcription factors converts human and murine fibroblasts to megakaryocyte progenitors with in vitro and in vivo functionality. MK progenitors can also be generated from disease-corrected fibroblasts, demonstrating that MK progenitors with clinical potential can be generated in vitro from somatic cells.

Pulecio et al., 2016, Cell Reports *17*, 671–683
October 11, 2016
http://dx.doi.org/10.1016/j.celrep.2016.09.036

Cell Reports
Article

Direct Conversion of Fibroblasts to Megakaryocyte Progenitors

Julian Pulecio,[1,2,*] Oriol Alejo-Valle,[1] Sandra Capellera-Garcia,[3] Marianna Vitaloni,[1] Paula Rio,[4,5] Eva Mejía-Ramírez,[1] Ilaria Caserta,[1] Juan A. Bueren,[4,5] Johan Flygare,[3] and Angel Raya[1,2,6,7,*]
[1]Center of Regenerative Medicine in Barcelona (CMRB), Barcelona Biomedical Research Park, Dr. Aiguader 88, 08003 Barcelona, Spain
[2]Center for Networked Biomedical Research on Bioengineering, Biomaterials and Nanomedicine (CIBER-BBN), 28029 Madrid, Spain
[3]Department of Molecular Medicine and Gene Therapy, Lund Stem Cell Centre, Lund University, 22184 Lund, Sweden
[4]Division of Hematopoietic Innovative Therapies, Centro de Investigaciones Energéticas, Medioambientales y Tecnológicas and Centro de Investigación Biomédica en Red de Enfermedades Raras (CIEMAT/CIBERER-ISCIII), 28040 Madrid, Spain
[5]Advanced Therapies Unit, I.I.S. Fundación Jiménez Díaz (UAM), 28040 Madrid, Spain
[6]Institució Catalana de Recerca i Estudis Avançats (ICREA), 08010 Barcelona, Spain
[7]Lead Contact
*Correspondence: jpulecio@cmrb.eu (J.P.), araya@cmrb.eu (A.R.)
http://dx.doi.org/10.1016/j.celrep.2016.09.036

SUMMARY

Current sources of platelets for transfusion are insufficient and associated with risk of alloimmunization and blood-borne infection. These limitations could be addressed by the generation of autologous megakaryocytes (MKs) derived in vitro from somatic cells with the ability to engraft and differentiate in vivo. Here, we show that overexpression of a defined set of six transcription factors efficiently converts mouse and human fibroblasts into MK-like progenitors. The transdifferentiated cells are CD41$^+$, display polylobulated nuclei, have ploidies higher than 4N, form MK colonies, and give rise to platelets in vitro. Moreover, transplantation of MK-like murine progenitor cells into NSG mice results in successful engraftment and further maturation in vivo. Similar results are obtained using disease-corrected fibroblasts from Fanconi anemia patients. Our results combined demonstrate that functional MK progenitors with clinical potential can be obtained in vitro, circumventing the use of hematopoietic progenitors or pluripotent stem cells.

INTRODUCTION

Transplantation of in-vitro-generated autologous megakaryocytes (MKs) has been proposed as a suitable alternative to conventional transfusions of allogeneic platelets to limit both alloimmunization and infection risks (Cho, 2015). MKs are responsible for the production of platelets. MKs are derived from hematopoietic stem cells (HSCs) in a process known as megakaryopoiesis, which consists of a series of events that can be divided in two steps: differentiation and maturation. Differentiation occurs after HSCs proliferate and commit to the myeloid lineage, giving rise to common myeloid progenitors that differentiate into bipotent megakaryocyte-erythrocyte progenitors (MEPs) (Pang et al., 2005). In turn, MEPs give rise to MK and erythroid progenitors. A subsequent differentiation step toward the MK lineage is mainly driven by thrombopoietin (TPO) and can be traced by the loss of the pan-hematopoietic marker CD45 and the appearance of the fingerprint of the MK lineage, the integrin αIIb or CD41. On the other hand, MK maturation involves cellular polyploidyzation and the development of a complex system of membranes that are the scaffolds for the formation of the proplatelets and subsequent platelets (Debili et al., 1996; Patel et al., 2005).

Several studies have identified a set of transcription factors (TFs), including TAL-1, RUNX1, ERG, LMO2, FLI1, and GATA-2, which are essential throughout hematopoiesis (Doré and Crispino, 2011; Loose et al., 2007). In the context of MEP differentiation, a complex interplay among C-MYC, FOG1, GATA1, GATA2, RUNX1, and SCL determines the commitment to a specific lineage (Tijssen et al., 2011). In particular, it has been shown that the upregulation of GATA2, RUNX1, and C-MYC represses the erythroid differentiation program and promotes the differentiation toward MK progenitors (Guo et al., 2009; Kuvardina et al., 2015). Likewise, terminal megakaryocytic differentiation is controlled by other TFs, including p45NFE2, MAF-G, and MAF-K, which form a protein complex that regulates the expression of platelet-characteristic proteins such as B-tubulin class VI and thromboxane synthase (Lecine et al., 2000; Shivdasani et al., 1995; Wang et al., 1986).

So far, platelets have been obtained from HSCs (Sim et al., 2016), although the availability of these cells in patients with bone marrow failure (BMF) syndromes is very limited (Ceccaldi et al., 2012). Similar approaches have been pursued from induced pluripotent stem cells (iPSCs) (Feng et al., 2014; Nakamura et al., 2014), although the low efficiencies of the reprogramming and differentiation protocols, in addition to the time required for each step, are current limitations for their clinical implementation in chronical platelet-deficit conditions (Cho, 2015). A revolutionary alternative to the classical procedures based on platelet transfusion therapies consists of the transplantation of MK progenitors able to engraft and release functional platelets

into the circulation (Fuentes et al., 2010; Wang et al., 2015). These results encourage the search for suitable protocols to generate patient-specific MK progenitors in vitro with clinical potential as an alternative to classical procedures of platelets transfusion from allogeneic donors.

As an alternative to somatic cell reprogramming and subsequent iPSC differentiation, the generation of blood cells by direct conversion strategies has proved to be a faster and more efficient way to convert somatic cells into terminally differentiated cells bypassing the pluripotent state (Ebina and Rossi, 2015; Xu et al., 2015). Recently, our groups have shown that the overexpression of a set of TFs, including *Gata1*, *Tal-1*, *Lmo2*, and *c-Myc*, directly converts human and murine fibroblasts into erythroid progenitors with the ability to express both fetal and adult globins (Capellera-Garcia et al., 2016). Considering these results in the context of TFs known to be important for MEP differentiation, we hypothesized that the transdifferentiation process could be skewed to favor the megakaryocytic lineage under specific conditions that recapitulate the differentiation events observed in vivo.

In this study, we demonstrate that overexpression of *Gata2* and *Runx1* in combination with the TF core (*Gata1*, *Tal-1*, *Lmo2*, and *c-Myc*) directly converts human and murine fibroblasts into $CD41^+$ cells resembling bona fide MK progenitors in vitro. When transplanted into immunocompromised mice, MK-like progenitors were able to engraft and differentiate into functional MKs capable of producing $CD41^+/CD42^+$ platelets. The relevance of this approach has been also demonstrated in a clinically relevant BMF disease model by converting gene-corrected fibroblasts from Fanconi anemia (FA) patients to MK-like cells.

RESULTS

Gata2 and Runx1 Bias the Direct Conversion of Human Fibroblasts to MK-like Progenitors

A recent study showed that human and murine fibroblasts can be directly converted to erythroid progenitors when a set of murine TFs composed of *Gata1*, *Tal-1*, *Lmo2*, and *c-Myc* (GTLM) is overexpressed in culture conditions that include the presence of erythropoietin (EPO) (Capellera-Garcia et al., 2016). Due to the common origin of erythroid and MK progenitors, we wondered if this system could be a starting point for the generation of MK cells from human somatic cells. Thus, we tested if the addition of TPO to the culture medium could bias the cellular conversion toward the MK lineage. To test this hypothesis, fibroblasts from two independent healthy donors were retrovirally transduced with the four murine TFs (GTLM) or with "all minus one" combinations in the presence of both EPO and TPO (Figures 1A and S1A). Thereafter, we monitored the presence of $CD235^+$ (early erythroid marker) and $CD41^+$ (early MK marker) cells during 12 days. We observed that the overexpression of GTLM caused the emergence of large rounded cells expressing CD41 or CD235, starting at day 4 and reaching at day 12 percentages of 10.9% ± 1.4% and 7.4% ± 3.3%, respectively (Figure 1B). Excluding a single factor from the GTLM cocktail was enough to completely block the generation of $CD41^+$ cells (Figure S1A).

These results encouraged us to search for additional TFs that would boost the differentiation toward the MK lineage. Several groups have demonstrated that GATA2 and RUNX1 play an essential role in the progression of MEP differentiation toward the MK lineage and subsequent MK maturation (Kuvardina et al., 2015; Tijssen et al., 2011). Hence, we decided to test if the addition of *Gata2* and/or *Runx1* to the TF cocktail would increase the efficiency of the conversion process.

Following the previous strategy to detect $CD41^+$ and $CD235^+$ cells, we observed that addition of each single factor *Runx1* or *Gata2* to the GTLM cocktail did not cause significant effects on the percentages of conversion ($p > 0.05$, $n = 3$). However, addition of both *Gata2* and *Runx1* to the GTLM cocktail resulted in a significant increase in the percentage of $CD41^+$ cells after 12 days (21.14% ± 3.6% compared to 10.91% ± 1.4% for GTLM alone, $n = 3$, $p < 0.05$) (Figure 1B). Interestingly, $CD41^+$ cells did not co-express CD34 or CD45 markers, suggesting a direct conversion process in which the generation of intermediate hematopoietic progenitors is omitted (Figure S1C).

The presence of $CD41^+$ cells prompted us to search for culture conditions that would enable the generation of MK progenitors from human fibroblasts. We hypothesized that the addition of cytokines, molecules, and factors reported to support the culture of MKs derived from $CD34^+$ cells (Emmrich et al., 2012) would increase the efficiency of the transdifferentiation. To test this, we followed two schemes of transdifferentiation. The first strategy was based on a two-phase differentiation system where an initial basal medium with TPO, interleukin-3 (IL-3), and stem cell factor (SCF) was replaced at day 4 for a more definitive medium (MK medium) including IL-6, IL-9, Rho-associated coiled-coil containing protein kinase (ROCK) inhibitor, low-density lipoprotein (LDL), and nicotinamide. The second strategy consisted of culturing the cells with the MK medium from the beginning of the conversion process (Figure 1C).

We monitored the percentage of $CD41^+$ and $CD41^+/CD42^+$ at days 4, 8, and 12 after transduction. We observed that the sole use of the MK medium from the beginning of the culture caused a significant increase in the efficiency of conversion at both day 8 and day 12 ($p < 0.001$ and $p < 0.05$, $n = 3$), producing a higher number of $CD41^+$ cells (~70%) after 12 days than the two-phase strategy (~40%). More importantly, we detected the presence of $CD41^+/CD42^+$ cells (a hallmark of mature MKs) after 8 days in culture, although with low efficiency (~1.5%) (Figure 1D). Remarkably, we observed a low variability in the efficiency of the transdifferentiation to $CD41^+$ cells between experiments regardless of the fibroblast source (Table S1) and a clear reduction in the percentage of $CD41^+$ cells obtained after 12 days with the GTLM cocktail (Figure S1D). Likewise, the culture of non-transfected fibroblasts with the MK medium was not enough to foster the conversion toward $CD41^+$ cells (Figure S1B).

Next, we analyzed the gene expression profile over the conversion process of $CD41^+$ cells obtained with the GTLM or the $GTLM^+$ *Runx1/Gata2* TF cocktail and compared it to MK progenitors ($CD34^+/CD41^+$ and $CD41^+/CD42^+$) derived in vitro from cord blood $CD34^+$ cells (Pineault et al., 2013) (Figure S2A). We observed that gene expression levels of isolated $CD41^+$ cells after 12 days of induction with $GTLM^+$ *Runx1/Gata2* TF cocktail resembled the expression profile of bona fide MK progenitors

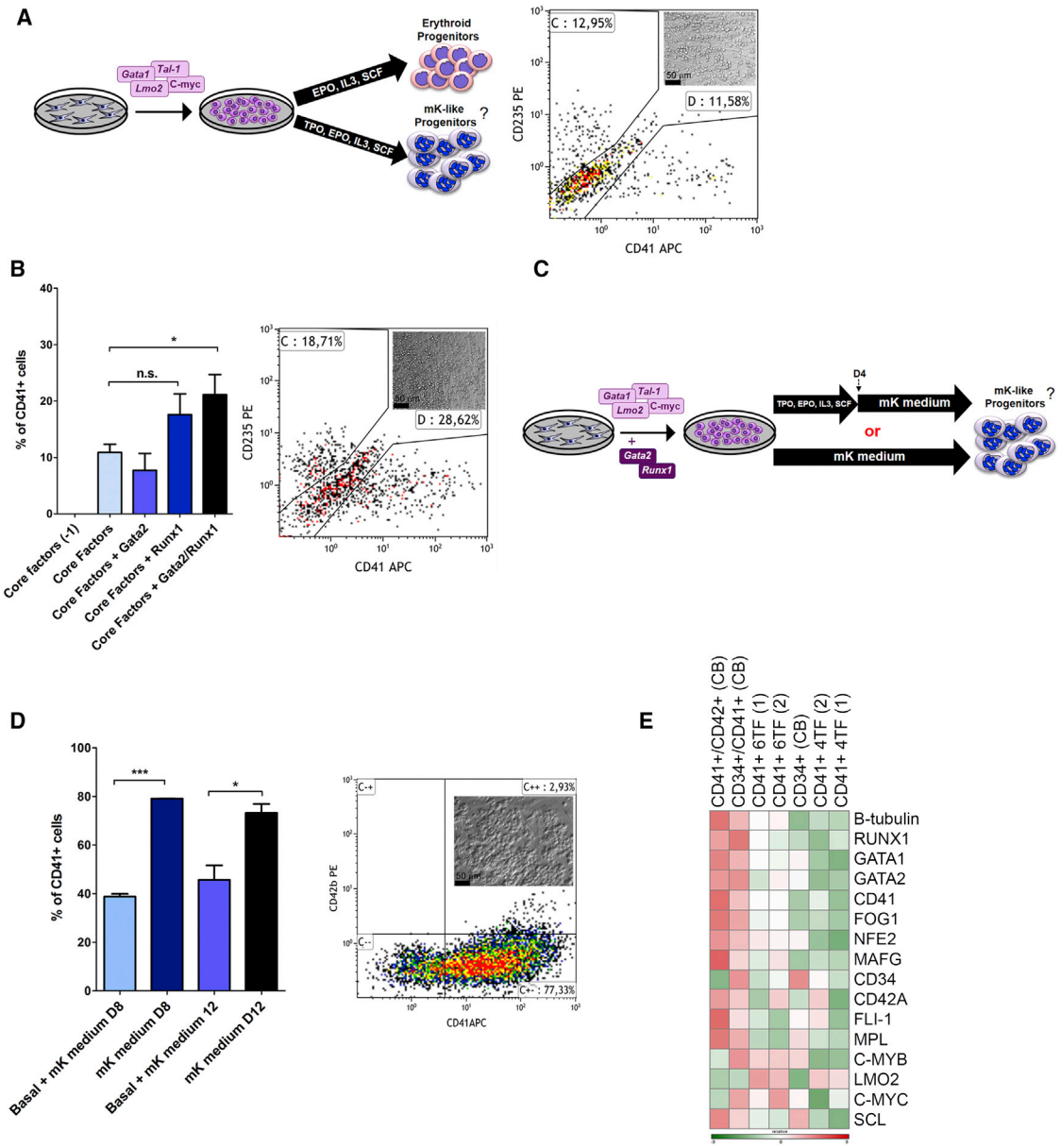

Figure 1. Gata2 and Runx1 Bias the Direct Conversion of Human Fibroblasts to MK-like Cells

(A) Diagram of the strategy used to obtain megakaryocytes (MKs) from human fibroblasts, based on the overexpression of a cocktail of GTLM TFs, in the presence of EPO and TPO (left). Transduction of human fibroblasts with the four core factors cultured with TPO and EPO causes the conversion toward $CD41^+$ and $CD235^+$ cells. Representative dot plot and cell culture pictures after 12 days are shown (right).

(B) The effect of the addition of Gata2 and Runx1 (single factor and combined) to the TF cocktail was tested. Transdifferentiation percentages were calculated for the different combinations of factors (left) ($p < 0.05$, $n = 3$). Error bars represent SEM. The appearance of round cells and higher percentages of $CD41^+$ cells (right) were observed when fibroblasts were transduced with GTLM + *Gata2* and *Runx1*.

(C) Diagram of the strategy used to enhance the percentage of differentiation toward MK-like progenitors based on the transduction of six TFs and two culture conditions designed to sustain the megakaryopoiesis.

(D) Bar graphs illustrating a significant increase in the percentage of $CD41^+$ cells at days 8 and 12 of conversion, when MK medium was used (left) ($p < 0.001$, $n = 6$ with two independent fibroblast lines). Error bars represent SEM. Representative dot plot and cell culture picture showing the presence of $CD41^+/42^{lo+}$ events after 12 days in culture, when cells were converted using the six-TF cocktail and MK medium (right).

(E) Gene expression analysis by qRT-PCR of two independent lines of fibroblasts (1 and 2) after overexpression of GTLM (4F) versus GTLM + *Runx1*/*Gata2* (6F) was studied and compared to MK progenitors derived in vitro from $CD34^+$ cord blood (CB) cells. Gene expression analysis was from four independent experiments. Positive controls were populations from CB progenitors cultured and differentiated in vitro. Relative heatmap scale is shown.

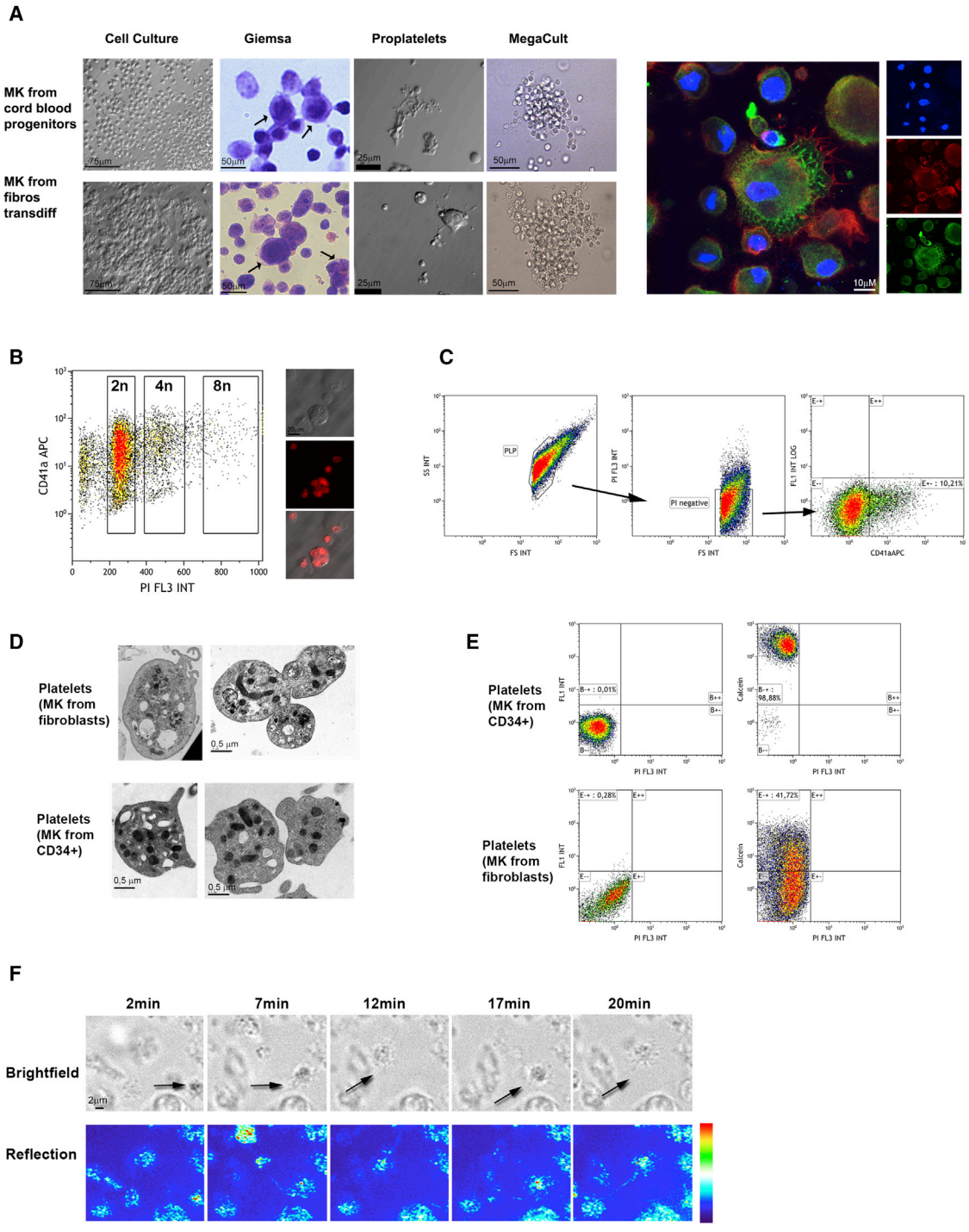

Figure 2. Transdifferentiated MK-like Cells Functionally Resemble Bona Fide MKs

(A) CD41^{+} human transdifferentiated fibroblasts were sorted after 12 days, and MK functionality was analyzed in culture. Shown are MK-like cells with polylobulated nuclei detected by Giemsa staining (indicated by arrowheads), a representative phase-contrast image of proplatelet-like structures found in the cell culture, and CFU-MKs detected by MegaCult assays (bottom). Corresponding positive controls from MKs derived from cord blood progenitors are shown (top). Immunofluorescence assays revealed the presence of MK-like cells expressing B-tubulin class VI (green), actin (phalloidin, red), and DAPI (blue) (right).

(B) Ploidy profile of CD41^{+} converted cells sorted after 1 week in culture. Representative pictures of the stained cells with propidium iodide (PI) showing a polylobulated nucleus are shown (right).

(C) Gating strategy used to study the presence of platelets produced in vitro, based on the presence of small PLPs PI^{-}/CD41^{+}.

(legend continued on next page)

(Figure 1E). Detailed analysis of these data show significant upregulation of genes specifically expressed in mature MKs, such as B-tubulin class VI, CD42a, FOG1, and p45NF-E2, when the fibroblasts were transduced with the GTLM $^{+}$ *Runx1/Gata2* TF cocktail compared to the ones transduced with the GTLM cocktail (Figure S1E). Importantly, overexpression of the murine TFs had a strong impact on the expression levels of their endogenous human counterparts.

In Vitro Differentiation of MK-like Progenitors Derived from Human Fibroblasts

We next tested if the CD41^{+} cells obtained after transdifferentiation of human fibroblasts with the GTLM $^{+}$ *Runx1/Gata2* functionally resembled bona fide MK-like progenitors derived in vitro. We isolated and analyzed CD41^{+} cells present after 12 days of transdifferentiation with the six-TF cocktail and the MK medium. In these isolated cultures, we detected the presence of large cells with polylobulated nuclei and the occasional presence of proplatelet-like structures. Likewise, by immunostaining analysis, we detected the presence of MK-like cells with a high expression of tubulin beta 1 class VI, an exclusive feature of MKs capable of producing platelets (Figures 2A and S2B). In parallel, we tested the ability to generate MK colony-forming units (CFU-MK) by MegaCult assays and we observed the emergence of similar numbers of CD41^{+} colonies after 14 days compared with MK progenitors derived from cord blood (Figures 2A and S1F). We also tested the presence of multipotent progenitors of non-megakaryocytic lineages in bulk cultures of fibroblasts transdifferentiated with GTML or with the six-TF cocktail, using standard MethoCult assays, and could not detect hematopoietic colonies after 14 days in either condition (n = 4; data not shown). In addition, we analyzed the nuclear content of the converted cells and detected the presence of CD41^{+} cells with ploidies reaching $\leq$8N (Figures 2B and S2B). Remarkably, all the characteristics above mentioned were absent in cultures of human fibroblasts transduced with the GTLM cocktail without *Runx1/Gata2* (Figure S1G).

Next, we wondered if the MK-like induced cells obtained from human fibroblasts could produce platelets in vitro. Thus, we recovered the platelet-like particle (PLP)-enriched fraction from the supernatant of the cell cultures and checked for the presence of CD41^{+} events. We detected the appearance of CD41^{+}/propidium iodide (PI)$^{-}$ PLPs in the supernatants of cells converted with the six TFs and cultured with MK medium (Figure 2C). The presence of platelets was corroborated by transmission electron microscopy (TEM) and compared to platelets derived in vitro from cord blood progenitors (Figure 2D). The low numbers of PLPs produced in vitro advised against the use of standard aggregation tests. However, we tested the functionality of the PLPs by performing previously standardized tests, such as spreading on activated glass and P-selectin expression (Feng et al., 2014), based on the presence of vital (calcein^{+}) platelets in the cell cultures (Figure 2E). We observed that PLPs derived in vitro were able to spread on activated glass and form "filopodia-like" membrane protrusions resembling the early stages of aggregation as observed in the control platelets (Figures 2F and S2D; Movies S1 and S2). In addition, we detected the presence of vital platelets expressing CD62p before agonist challenge. However, the percentage of CD62p^{+} platelets did not change after incubation with a mix of thrombin and ADP (see Experimental Procedures and Supplemental Experimental Procedures). In contrast, a low percentage of platelets derived in vitro from cord blood progenitors increased the expression of CD62p upon agonist challenge (Figure S2C).

Direct Conversion of Mouse Fibroblasts to MK-like Progenitors

Once we observed that human fibroblasts could be converted into functional MK-like progenitors, we decided to test this protocol with mouse fibroblasts, since the murine model is more amenable to in vitro and in vivo functional analyses (Sykes and Scadden, 2013).

We retrovirally transduced the set of four TFs (GTLM) and six TFs (GTLM plus *Runx1/Gata2*) into mouse embryonic fibroblasts (MEFs) cultured with the MK medium. We monitored the presence of hematopoietic (CD45), erythroid (Ter-119), and/or megakaryocytic (CD41) cells for 12 days. The appearance of large rounded cells at day 4 coincided with the emergence of CD41^{+}/CD45^{-} cells ($\sim$8%) and lasted until day 12 in both conditions. In contrast with the results obtained with human fibroblasts, no erythroid cells were found at any time point during the conversion process (Figures 3A and S3A).

Due to the relatively low percentages of differentiation and looking for a pure population to characterize the phenotype of the MK-like progenitors in culture, we FACS sorted the CD41^{+} cells after 12 days of differentiation generated by both strategies (GTLM and GTLM $^{+}$ *Runx1/Gata2)*. Remarkably, only the CD41^{+} population produced by the overexpression of the six TFs gave rise to an expandable population that was kept in culture for at least 2 weeks and reached a $\sim$30-fold increase in the number of CD41^{+} cells, while high-purity cultures ($\sim$70%) were maintained (Figures 3A and 3B). Next, we proceeded to study the gene expression profile of the CD41^{+} purified population and compared it to MK progenitors from murine bone marrow samples (CD34^{+}/CD41^{+}) and to CD41^{+} populations obtained during the transdifferentiation. We detected a gradual increase in the expression of MK-specific genes such as *Nf-e2*, *B-tubulin VI*, *CD41*, and *CD42*b, *Mpl*, and *Fli-1* over the conversion process until they reached levels of expression similar to the positive controls. As observed in the human model, the use of the GTLM cocktail produced significantly fewer CD41^{+} cells with a gene

(D) PLP produced by MK-like progenitors derived from human fibroblasts were analyzed by TEM and compared to PLP produced in vitro from MK derived from CD34^{+} cells. The presence of characteristic platelets features such as alpha and dense granules is observed.

(E) Representative dot plot images displaying the presence of calcein-positive platelets are shown.

(F) Formation of membrane protrusions distinctive of the early stages of platelets aggregation was studied by adhesion of PLPs to activated glass. Images from time-lapse experiments performed for 20 min are shown. The morphology of the platelets is followed by bright-field images (top) and light reflection (bottom) (intensity scale is shown).

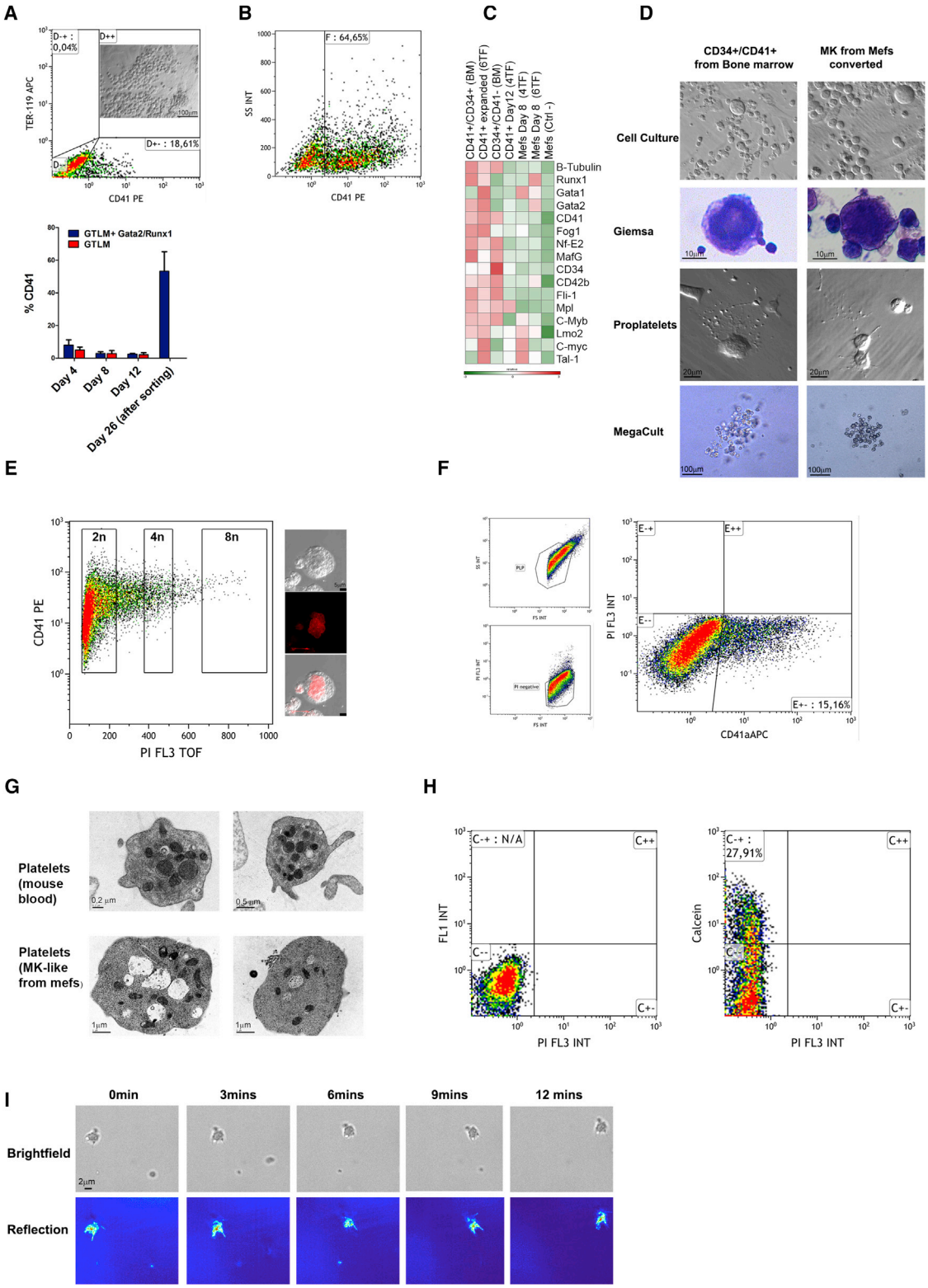

Figure 3. Conversion of Mouse Fibroblasts into MK-like Progenitors In Vitro

(A) MEFs were retrovirally transduced with the four-TF and six-TF cocktails, cultured with MK medium, and the presence of erythroid/MK cells was monitored over 12 days. Dot plot revealing the percentage of $CD41^{+}$ and bright-field pictures from a culture of converted fibroblasts with the GTLM +

(legend continued on next page)

expression profile distant from bona fide MK progenitors (Figures 3C and S3C).

We next tested if the expandable population of CD41$^+$ cells obtained after MEF transdifferentiation with the GTLM $^+$ *Runx*1/*Gata2* functionally resembled bona fide MK progenitors. When we analyzed in detail the culture of the purified CD41$^+$ population, we could detect large rounded cells with prominent polylobulated nuclei. Interestingly, we could observe the occasional appearance of proplatelet-like structures, an indication that MK maturation was occurring in vitro (Figure 3D). Then, we proceeded to functionally test the progenitor capacity of the CD41$^+$ transdifferentiated cells. By measuring the cellular ploidies, we observed that the purified CD41$^+$ population contained polyploid cells reaching $\leq$8N (Figure 3E). Moreover, the functional characterization of MK-like progenitors in standard MegaCult assays revealed the presence of CFU-MKs after 12 days in culture, resembling the results obtained with MK endogenous progenitors from bone marrow (Figure 3D).

Next, we wondered if the MK-like cells obtained from MEFs could produce platelets in vitro. For this purpose, we recovered the supernatant fraction of CD41$^+$ expandable cultures and checked the presence of PLPs by flow cytometry. We identified a CD41$^+$/PI$^-$ PLP population in the expanded cultures of purified CD41$^+$ cells converted with the six TFs (Figure 3F). Then, using TEM assays, we corroborated the presence of platelets in the cell cultures, which resembled the morphology of bona fide platelets from peripheral murine blood (Figure 3G). Next, as observed with human PLPs, we detected the presence of vital platelets (Figure 3H) able to spread on activated glass and to form membrane filopodia-like protrusions (Figure 3I; Movie S3). Last, we looked for the expression of CD62p by platelets derived in vitro after challenging them with agonists. As observed in the human model, we detected a similar population of CD62p$^+$ PLPs in the murine cell cultures that did not increase upon agonist challenge (Figure S3D).

MK-like Progenitors Are Able to Engraft and Differentiate In Vivo

Then, we decided to evaluate the functionality of the mouse MK-like progenitors by testing their ability to engraft and differentiate in vivo. In order to track the presence of MKs and platelets in vivo, we added a GFP retrovirus to the transdifferentiation TF cocktail. In these experiments, we intravenously injected 1 × 10^5 CD41$^+$/GFP$^+$/CD42$^-$ MK-like progenitors into sublethally irradiated NSG mice. We then monitored weekly the presence of CD41$^+$/GFP$^+$/CD42$^+$ mature MKs in all the possible niches where the megakaryocytic progenitors could engraft and differentiate (e.g., spleen, lungs, bone marrow, and peripheral blood). As a positive control, we used purified CD34$^+$/CD41$^+$ cells from non-irradiated NSG donors transduced with GFP lentiviruses (Figure 4A).

After the first week, we detected by flow cytometry a CD41$^+$/GFP$^+$/CD42$^+$ population in the peripheral blood of 75% of transplanted mice (16.7% ± 4.7% of the total CD41$^+$ population), which was also confirmed by fluorescence microscopy and qRT-PCR. An equivalent population of engrafted and differentiated cells was detected in mice transplanted with control cells (Figures 4B and S4A). 2 weeks post-transplantation, we detected a cluster of CD41$^+$/GFP$^+$ cells engrafted in the bone marrow and the lungs of several mice (2.2% ± 0.7% and 7.2% ± 2.8% of engraftment compared to the total CD41$^+$ population, respectively; n = 9). Remarkably, a subpopulation of CD41$^+$/GFP$^+$ cells also expressed CD42 (13.5% ± 4.6% and 21.2% ± 6.9% relative to the total CD41$^+$/CD42$^+$ population in bone marrow and lungs, respectively) indicating that the MK-like progenitors derived in vitro were able to differentiate into CD41$^+$/CD42$^+$ MKs (Figures 4C and 4D). The presence of GFP$^+$ cells was corroborated by qRT-PCR (Figure S4C). As expected from transplanted MK progenitors, the percentage of engraftment decreased over time, but we could still detect CD41$^+$/GFP$^+$/CD42$^+$ cells in the bone marrow of one out of five mice analyzed 3 weeks after transplantation (0.7% of total CD41$^+$/CD42$^+$ cells). Notably, we did not detect GFP$^+$ cells in peripheral blood or lungs after 3 weeks in any of the transplanted mice. These results are in line with the observed values of engraftment for mice transplanted with control cells (Figure S4B).

Finally, we analyzed the samples for the presence of PLPs derived from the exogenous MK-like progenitors and detected a population of CD41$^+$/GFP$^+$ cells in the PLP fraction of several mice after 2 weeks (9.9% ± 3.9% in lungs and 7.3% ± 3.2% in bone marrow of the total CD41$^+$ population; n = 9; Figures 4E and 4F). Overall, converted MK-like progenitors displayed a

Runx1/Gata2 cocktail after 4 days is shown (top). Graph bars showing the percentage of CD41$^+$ cells along the transdifferentiation process (n = 5) (bottom). Error bars represent SEM.

(B) Representative dot plot of the percentage of CD41$^+$ cells of a culture derived from MEFs with six TFs after 2 weeks of expansion.

(C) Gene expression analysis by qRT-PCR of the converted cells after overexpression of the six-TF and four-TF cocktails was performed and compared to MK endogenous progenitors isolated from murine bone marrow samples (CD41$^+$/CD34$^+$ and CD34$^+$/CD41$^-$). Relative heatmap scale is shown.

(D) The functionality of the expandable population of CD41$^+$ MK-like murine progenitors was analyzed in culture. Shown are MK-like cells with polylobulated nuclei detected by Giemsa staining, a representative phase-contrast image of proplatelet-like structures found in the cell culture, and CFU-MKs detected by MegaCult assays (right). Corresponding positive controls from MKs derived from bone marrow progenitors are shown (left).

(E) Ploidy profile of CD41$^+$ converted cells sorted after 2 weeks in culture. Representative pictures of the cells stained with PI showing a polylobulated nucleus are shown (right).

(F) Gating strategy used to study the presence of platelets produced in vitro by MK-like murine progenitors, based on the presence of small PLPs (PI$^-$/CD41$^+$).

(G) PLPs produced by MK-like progenitors derived from murine fibroblasts were analyzed by TEM and compared to PLPs isolated from mouse peripheral blood. The presence of characteristic platelets features such as alpha and dense granules is observed.

(H) The presence of vital platelets in the culture produced by the expandable MK-like murine cells was analyzed by calcein assays. Representative dot plots are shown.

(I) Formation of membrane protrusions distinctive of the early stages of platelet aggregation was studied by adhesion of PLPs to activated glass. Images from time-lapse experiments performed over 12 min are shown. The morphology of the platelets is followed by bright-field images (top) and light reflection (bottom).

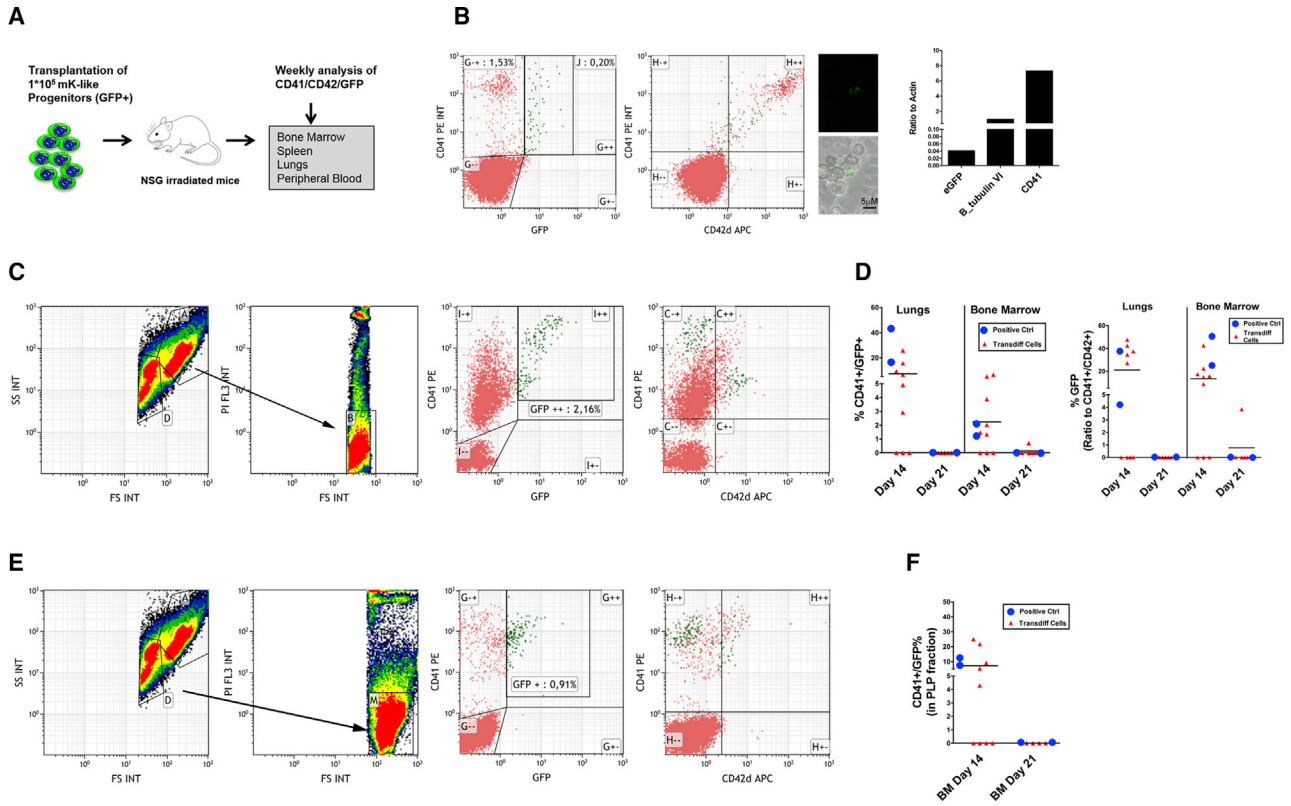

Figure 4. In Vitro Engraftment of MK-like Progenitors into NSG Mice

(A) Diagram of the strategy used to evaluate the ability to engraft and produce platelets of the murine MK-like progenitors generated in vitro. CD41$^+$/GFP$^+$/CD42$^-$ cells obtained after 12 days of conversion were injected into sub-lethally irradiated NSG mice, and the presence of exogenous MKs/platelets was monitored weekly.

(B) Dot plots indicating the presence of CD41$^+$/GFP$^+$ cells (green dots) and CD41$^+$/CD42$^+$/GFP$^+$ cells in the peripheral blood after 1 week of transplantation. Engraftment percentages, taking as a reference the total number of cells, are shown inside the dot plot. The presence of GFP$^+$ cells in the peripheral blood was corroborated by optical microscopy and qRT-PCR of the blood samples (right).

(C) Gating strategy to detect the presence of GFP$^+$/CD41$^+$/CD42$^+$ cells in the bone marrow and lungs 2 weeks after transplantation. Representative dot plots of a bone marrow sample from a mouse transplanted with transdifferentiated MK-like progenitors generated in vitro are shown (green dots correspond to GFP$^+$ cells).

(D) Scatterplots depict the percentage of engraftment of CD41$^+$/GFP$^+$ (left) and differentiation to CD41$^+$/CD42$^+$/GFP$^+$ (right) cells in the lungs and the bone marrow after several weeks (see Experimental Procedures) for each mouse. Mice transplanted with transdifferentiated cells (red triangles) and positive controls (blue dots) are plotted. Black lines indicate mean percentage of engraftment for mice transplanted with the transdifferentiated cells.

(E) Gating strategy to detect the presence of GFP$^+$/CD41$^+$/CD42$^+$ platelets in the bone marrow and lungs 2 weeks after transplantation. Representative dot plots of the same bone marrow sample analyzed in (D) from a mouse transplanted with transdifferentiated MK-like progenitors generated in vitro are shown (green dots correspond to GFP$^+$ PLPs).

(F) Scatterplots depict the percentage of CD41$^+$/GFP$^+$ platelets in the bone marrow after several weeks for each mouse (see Experimental Procedures). Mice transplanted with transdifferentiated cells (red triangles) and positive controls (blue dots) are plotted. Black lines indicate mean percentage of GFP$^+$ platelets (compared to the total PLP population) for mice transplanted with transdifferentiated cells.

capacity to engraft and differentiate comparable to that of positive control cells (Figures 4D, 4F, and S4). Altogether, this set of results shows that MK-like progenitors generated in vitro by the overexpression of GTLM $^+$ *Gata2/Runx1* are able to engraft and mature in vivo.

Direct Conversion of MK-like Progenitors from Fibroblasts of Fanconi Anemia Patients

To provide proof of concept for the clinical potential of our transdifferentiation protocol, we tested it in a context where the generation of functional MKs would be clinically relevant. FA is a disease in which thrombocytopenia frequently constitutes one of the earliest events of BMF (Pawlikowska et al., 2014; Río et al., 2002) and the number of HSCs is markedly reduced. In order to test our protocol, we used both uncorrected (GFP-FA) and gene-corrected fibroblasts (FANCA-FA) (see Experimental Procedures and Supplemental Experimental Procedures) from FA patients and compared their ability to differentiate into CD41$^+$ MK-like cells. To confirm the correction of FANCA-FA after transduction with the lentiviral vector PGK-FANCA, FANCD2 foci were analyzed by immunofluorescence after challenging the cells with mitomycin C (Figure S5A; see Experimental Procedures for details).

Both GFP-FA and FANCA-FA fibroblasts were able to produce CD41$^+$ cells in a way similar to that observed with healthy fibroblasts. However the percentage of MK-like cells was significantly higher in gene-corrected FA fibroblasts compared to GFP-FA fibroblasts (Figure 5A). Gene expression analysis of isolated CD41$^+$ cells after 12 days of conversion revealed that MK progenitors derived from gene-corrected FA fibroblasts reached similar expression levels compared to CD41$^+$ cells derived from healthy fibroblasts, while CD41$^+$ cells obtained from diseased fibroblasts barely differentiated from their starting population (Figures 5B and S5B). We next isolated the CD41$^+$ cells derived from GFP-FA and FANCA-FA fibroblasts and tested their functionality as performed for healthy fibroblasts. Only when the FA fibroblasts were gene-corrected we were able to detect the presence of large cells with polylobulated nuclei, pro-platelets, tubulin beta 1 class-VI-positive cells, polyploid cells ($\leq$8N), and CFU-MKs (Figures 5C, 5D, and S5C).

Finally, we analyzed the PLP fraction in MK-like cultures derived from GFP-FA and FANCA- FA fibroblasts in order to detect the presence of platelets. Remarkably, we were able to detect a CD41$^+$ PLP population only when FA fibroblasts were gene-corrected, although with lower efficiencies compared to healthy fibroblasts (Figure 5E). However, when we performed TEM, calcein assays, adhesion to activated glass, and activation upon agonist challenge experiments, we found that the platelets derived from FANCA-FA fibroblasts were roughly functionally equivalent to platelets derived from healthy fibroblasts (Figures 5F, 5H, and S5D; Movie S4).

DISCUSSION

Previous reports on direct reprogramming to hematopoietic lineages described the generation of rather primitive blood progenitors with a marked myeloid differentiation capacity (Batta et al., 2014; Ebina and Rossi, 2015; Pulecio et al., 2014; Szabo et al., 2010). In contrast, in this work we described a transdifferentiation approach designed to produce blood lineage-restricted progenitors. Here, we show that human and mouse fibroblasts can be transdifferentiated into MK-like progenitors by overexpressing six TFs. In-vitro-generated MK-like progenitors showed hallmarks of MK identity, including the ability to form MK colonies, generate proplatelet-like structures, and produce vital platelets in vivo, and, when challenged in vivo, to engraft and give rise to mature MKs and platelets.

Direct transdifferentiation of fibroblasts to mature MK-like cells was reported through overexpression of only three TFs (p45NF-E2, Maf-G, and Maf-K) (Ono et al., 2012). None of these factors alone or in combination had any significant effect on the efficiency of transdifferentiation to MK-like progenitors achieved with our system (data not shown). This suggests that the molecular mechanisms underlying cell-fate conversion in our approach compared to the previous one are independent. In this respect, we reasoned that direct conversion toward lineage-restricted progenitors, rather than terminally differentiated cells, would be advantageous for the megakaryocytic lineage, since mature MK have limited proliferation ability and engraftment potential. The benefits of generating progenitor-like cells by direct reprogramming have already been noted in other contexts, including neural (Han et al., 2012; Lujan et al., 2012; Ring et al., 2012), hepatic (Yu et al., 2013), and cardiac (Lalit et al., 2016) progenitors.

In order to respond to the demand of platelets, two strategies have been proposed. The first is the generation of functional clinical-grade platelets that could be banked and available for their immediate supply. This strategy has been previously described and is based on the differentiation of CD34$^+$ progenitors and/or iPSCs (Feng et al., 2014; Nakamura et al., 2014). On the other hand, clinical conditions causing a chronic deficit of platelets, such as the thrombocytopenia observed in FA patients, would require a different solution. In this scenario, the generation of engraftable MK progenitors would be an ideal tool to develop. In the light of this, the process of direct conversion described here, which takes only 12 days and generates MK-like progenitors able to differentiate and produce platelets in vivo with a ~30-fold expansion capacity, provides a practically feasible setup for clinical implementation.

Nonetheless, when we tested the ability to engraft of the human MK progenitors in vivo, we did not detect the presence of human CD41$^+$ cells after 2 weeks of transplantation (data not shown). A possible explanation for this could be that species-specific signals for maintaining a progenitor-like phenotype could not be fully recapitulated in the human system in vitro (Riddell et al., 2014) or provided by the mouse niche(s) upon transplantation. While further research will be necessary to characterize the species-specific requirements for maintaining a MK-like progenitor phenotype, our combined results demonstrate that the activation of the MK lineage program induced by overexpressing GTLM $^+$ *Runx1/Gata2* is conserved in both human and mouse fibroblasts.

While the main goal of this study was not to generate platelets in vitro with direct clinical applications, the functionality of the MK progenitors was corroborated when we detected vital platelets in the cell cultures of the transdifferentiated fibroblasts. However, the numbers and the functionality of the platelets observed suggests that future projects aiming to generate large-scale functional platelets in vitro would require specific culture systems to control for shear stress, temperature restrictions, and the use of metalloprotease inhibitors, among other conditions (Figures S1I, S3E, and S5E) (Sim et al., 2016; Wang et al., 2015).

Throughout hematopoiesis, TFs command the induction and maintenance of the expression of lineage-specific genes, as well as the suppression of competing gene expression programs (Orkin and Zon, 2008; Pimanda and Göttgens, 2010). TAL-1, RUNX1, GATA2, GATA1, and LMO2 make part of a cluster of TFs that are crucial to define and maintain HSC as well as MEP, erythroid, and MK identity (Loose et al., 2007; Robb et al., 1996; Tijssen et al., 2011). This occurs because identical sets of TFs may play opposing roles at different steps of lineage commitment depending on the specific cellular context in which they are expressed. In the context of forced cell-fate conversion, the role of these TFs may be modified and have a different effect on the cellular outcome (Graf and Enver, 2009).

Exogenously overexpressed TFs can act as activators or repressors depending on the epigenomic landscape and the relative amounts of the endogenous TFs expressed in the somatic cell to be reprogrammed (Vierbuchen and Wernig, 2011). In

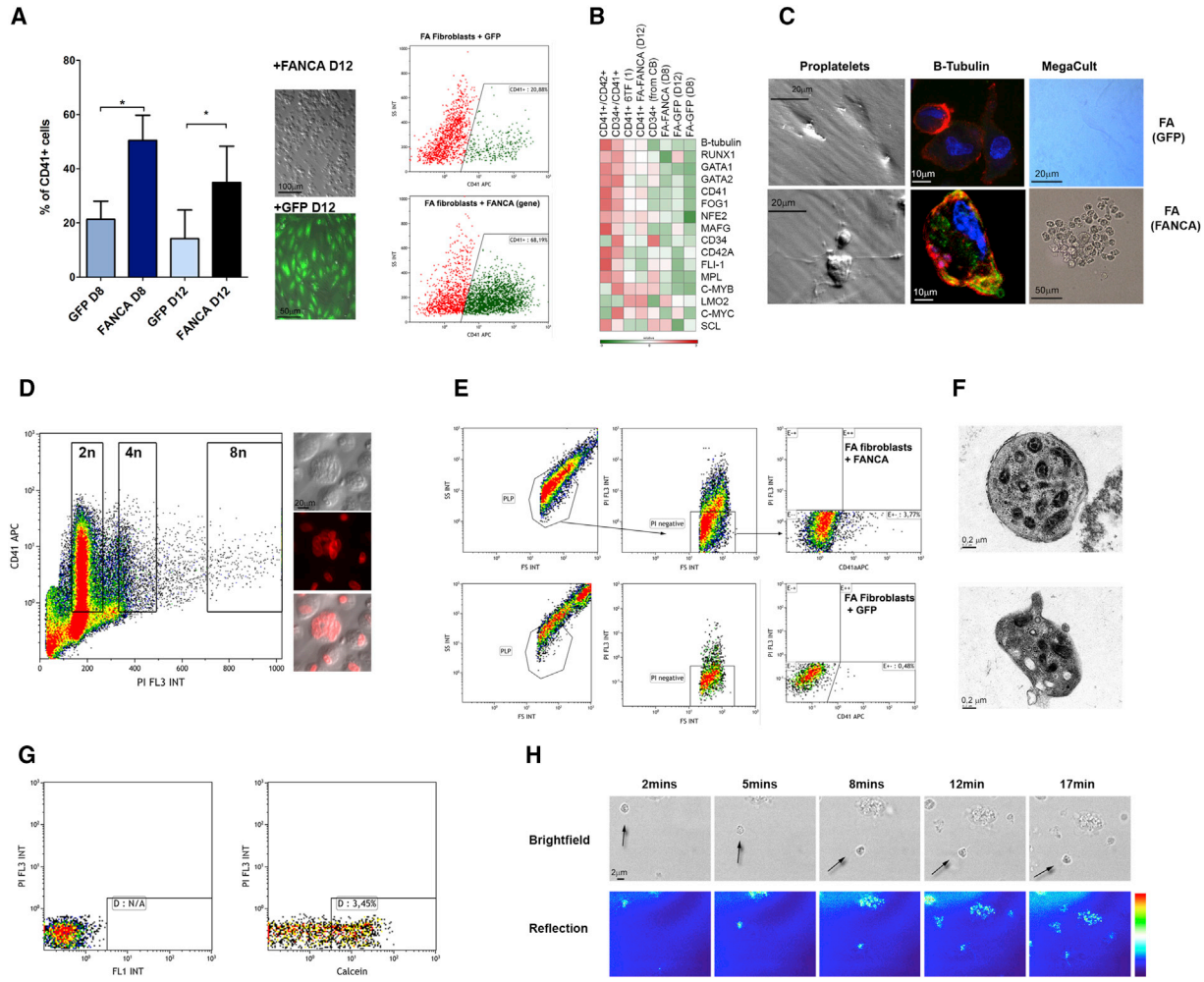

Figure 5. Conversion of Fanconi-Anemia-Corrected Fibroblasts into MK-like Progenitors In Vitro

(A) FA fibroblasts were gene corrected (FANCA) and compared to mock-infected (GFP) controls to test the suitability of our protocol in a clinical context. Bar graphs indicating the percentages of conversion to $CD41^+$ at days 8 and 12 are shown ($n = 4$, $p < 0.05$). Error bars represent SEM. Cell culture pictures after 12 days of culture for each condition are shown (middle). Representative dot plots of GFP-FA and FANCA-corrected cells at day 12 of conversion are shown (right).

(B) Gene expression analysis by qRT-PCR of the FANCA-corrected (FA-FANCA) and diseased (GFP-FA) fibroblasts converted after six-TF-cocktail overexpression was studied and compared to $CD41^+$ cells transdifferentiated from healthy fibroblasts and MK progenitors derived in vitro from $CD34^+$ cord blood cells. Relative heatmap scale is shown.

(C) $CD41^+$ cells generated from GFP-FA and FANCA-FA fibroblasts were sorted after 12 days, and MK functionality was analyzed in culture. Representative phase-contrast images of proplatelet-like structures found in the cell culture of gene-corrected FA fibroblasts, MK-like cells expressing B-tubulin class VI (green) and actin (phalloidin, red), and CFU-MKs detected by MegaCult assays are shown (bottom). Comparative images of the negative results obtained with GFP-FA $CD41^+$ cultures are shown (top).

(D) Ploidy profile of $CD41^+$ converted cells sorted after 1 week in culture. Representative pictures of the stained cells with PI showing a polylobulated nucleus are shown (right).

(E) Gating strategy used to study the presence of platelets produced in vitro, based on the presence of small PLP, $PI^-/CD41^+$, both in FANCA-FA (top) and GFP-FA (bottom) converted cell cultures.

(F) The presence of PLPs produced by MK-like progenitors derived from FANCA-corrected fibroblasts was corroborated by TEM images (see Figure 2D).

(G) The presence of vital platelets in the culture produced by gene-corrected FA fibroblasts was analyzed by calcein assays. Representative dot plots are shown (see Figure 2E).

(H) The formation of membrane protrusions distinctive of the early stages of platelet aggregation was studied by adhesion of PLPs to activated glass. Images from time-lapse experiments performed over 20 min are shown. The morphology of the platelets is followed by bright-field images (bottom) and light reflection (top) (Figure 2F).

this direction, we previously established that overexpression of GATA-1, TAL-1, LMO2, and C-MYC is sufficient to induce the conversion of fibroblasts to erythroid progenitors (Capellera-Garcia et al., 2016). Taking these observations into account, the results of our current study are consistent with previous reports that demonstrate that GATA2 and RUNX1 foster the generation of MK progenitors by occupying a set of shared promoter regions bound by GATA1 in erythroid progenitors. In the context of MK lineage specification, it has been demonstrated that GATA2 binds the active promoter regions shared with GATA1 and causes the repression of their targets through the interaction with additional TFs such as FOG1 (Huang et al., 2009; Tsai et al., 1994). Moreover, RUNX1 has been shown to interact with SCL, triggering the activation of FLI1 and recruiting a gene-activating complex to MK-related genes while repressing the erythroid program by inhibiting the activity of KLF1 (Kuvardina et al., 2015).

In addition to the instrumental role of TFs, instructions conferred by the culture conditions are essential to drive cell lineage conversion in direct transdifferentiation approaches (Daniel et al., 2016). The results of our study clearly show that this is the case for MK lineage conversion as well, since the sole addition of TPO to the culture medium led to the appearance of MK-like progenitors using a TF cocktail previously shown to activate the erythroid lineage (Capellera-Garcia et al., 2016). Further addition of cytokines and molecules that support MK maturation in vitro from cord blood progenitors (Emmrich et al., 2012) significantly increased the efficiency of the conversion of human fibroblasts. In an effort to provide proof of principle for the clinical applicability of the direct conversion strategy developed here, we reprogrammed fibroblasts from FA patients. FA is a BMF characterized by a reduced content of HSCs, which causes defective thrombocytopenia (Río et al., 2002), as well as impaired endomitosis during megakaryopoiesis (Pawlikowska et al., 2014). Our results indicate that prior gene complementation of FA fibroblasts with a healthy copy of the *FANCA* gene, significantly improved their ability to transdifferentiate to MK-like cells when compared to uncorrected FA fibroblasts. This is consistent with previous studies showing that *FANCA* is required for effective megakaryopoiesis of mouse HSCs (Pawlikowska et al., 2014). Although our results should be considered preliminary in the clinical context, they open the road to exploring further characterization and development of MK progenitors derived from gene-corrected fibroblasts from FA patients and from other diseases requiring platelet transfusion, especially in those cases in which the HSCs content is also affected.

The clinical translation of this approach would also require addressing several important shortcomings. Chief among them the issue of safety of the transdifferentiated cells should be thoroughly examined before any treatment of human patients is attempted. In this regard, the use of inducible systems or non-integrative delivery methods for achieving TF overexpression in fibroblasts should be developed, a goal that will undoubtedly benefit from the remarkable advances in the field of induced reprogramming to pluripotency (Brouwer et al., 2016; Schlaeger et al., 2015). In particular, mRNA reprogramming has been shown as an appealing alternative that conforms to the limitations imposed for clinical-grade procedures, without affecting the efficiency of reprogramming (Ebina and Rossi, 2015). In addition to the generation of autologous MK-like progenitors, the methods described here provide the foundation for future studies aimed at producing functional platelets in vitro using direct cell-fate conversion. Future studies on the direct reprogramming of fibroblasts to MK-like progenitors will be important for advancing the applicability of this approach.

EXPERIMENTAL PROCEDURES

Derivation of Mouse Embryonic Fibroblasts

All experiments involving animal subjects were conducted following procedures approved by the Ethics Committees on Experimental Animals of the Barcelona Biomedical Research Park. At least two 14.5 embryos were collected from CD1 mice decapitated while the liver was pulled out. Decapitated embryos were minced, treated with trypsin/EDTA 0.05% in presence of penicillin/streptomycin and after pipetting were incubated at 37°C for 15min. Cellular content was filtered with a 40-μm cell strainer, washed with complete DMEM (DMEM plus 10%FBS [Gibco] plus Glutamax [Invitrogen] plus 50 U/mL penicillin and 50 mg/mL streptomycin [Invitrogen]), and centrifuged at 1,200 rpm for 5 min at room temperature. The pellet was resuspended in complete DMEM and plated in a 15-cm dish. Cells were split once and mycoplasma tested.

Human Fibroblasts

Experiments involving the procurement and use of samples from human subjects were conducted after approval by the Institutional Review Board at Center of Regenerative Medicine in Barcelona (CMRB) and/or Centro de Investigaciones Energéticas, Medioambientales y Tecnológicas (CIEMAT). Two primary fibroblast lines were derived from human skin biopsy specimens obtained with informed consent from patients. For experiments with FA samples, skin fibroblasts were obtained from patient FA-707 after informed consent was signed. All three lines were negative for hematopoietic markers, including CD34. Fibroblasts were cultured in complete DMEM. All cell lines were maintained in an incubator (37°C, 5% CO_2), with media changes every second day.

Retroviral and Lentiviral Vector Production and Transduction

Coding regions for the candidate genes (*Lmo2*, *Gata1*, *Tal-1*, *c-Myc*, *Gata2*, and *Runx1* and EGFP) were amplified and cloned into pMXs retroviral vector backbone. For retrovirus production, 4×10^6 Phoenix-AMPHO cells were seeded in Opti-MEM (Gibco) and transfected with Fugene6 (Promega) DNA mix (3:1 ratio). Culture medium was switched to complete DMEM the day after; fresh virus productions were filtered through a 0.45-μm filter and were collected after 24 and 48 hr.

For the experiments with FA fibroblasts, vectors containing PGK-FANCA and PGK-EGFP were used to generate third-generation self-inactivating lentiviruses (LVs) pseudotyped with vesicular stomatitis virus-G protein (VSV-G) envelopes. Lentiviral particles were prepared by four-plasmid calcium phosphate-mediated transfection in 293T cells, essentially as previously described (Dull et al., 1998), and vector stocks were titrated (Charrier et al., 2011)

1×10^5 fibroblasts were plated in p6 wells and transduced for 24 hr with an MOI 20 of PGK-EGFP-LV as a control vector or PGK-FANCA-LV (González-Murillo et al., 2010). 24 hr later, cells were washed and used for trans-differentiation studies.

In Vivo Transplantation Experiments

100 μL PBS containing 100,000 $CD41^+/CD42^-/GFP^+$ in vitro transdifferentiated cells mixed with 100,000 unsorted cells isolated from the bone marrow of a healthy donor were injected into sub-lethally irradiated NSG mice (225 Gy) in the retro-orbital cavity. Blood samples were collected weekly. After 2–3 weeks, mice were sacrificed, and samples from peripheral blood, spleen, bone marrow, and lungs were collected. The presence of $CD41^+/CD42^+/GFP^+$ cells and platelets was evaluated by fluorescence-activated cell sorting (FACS) and corroborated by qRT-PCR and optical microscopy. 100,000 $CD34^+/CD41^+/GFP^+$ cells from syngeneic NSG donors were injected in positive-control experiments. Two rounds of experiments with a total of 23 mice were performed.

The percentage of engraftment was calculated as ($CD41^+/GFP^+$ cells/ $CD41^+$ cells) × 100) for each niche. The percentage of differentiation was calculated as ($CD41^+/CD42^+/GFP^+$ cells/ $CD41^+/CD42^+$ cells) × 100). The percentage of PLPs derived from engrafted MK-like cells was calculated as ($CD41^+/GFP^+$ PLPs/ $CD41^+$ PLPs) × 100).

Statistical Evaluation

Statistical analyses were performed using unpaired Student's t and Mann-Whitney tests (one-tailed, 95% confidence intervals) using GraphPad 5.0 (Prism). All data are presented as mean ± SEM and represent a minimum of three independent experiments with at least three technical replicates.

See Supplemental Experimental Procedures for a detailed description of the experimental design and reagents used in this study.

SUPPLEMENTAL INFORMATION

Supplemental Information includes Supplemental Experimental Procedures, five figures, one table, and four movies and can be found with this article online at http://dx.doi.org/10.1016/j.celrep.2016.09.036.

AUTHOR CONTRIBUTIONS

Conceptualization, J.P., J.F., and A.R.; Methodology; J.P., O.A.V., S.C.G., E.M.R., M.V., and I.C.; Formal Analysis, J.P., O.A.V, and A.R.; Investigation, J.P., O.A.V., S.C.G., M.V., E.M.R., and I.C.; Resources, S.C.G., P.R., J.A.B., and J.F.; Writing – Original Draft, J.P. and A.R.; Writing – Review & Editing, all authors; Funding Acquisition, J.A.B., J.F., and A.R.; Supervision, J.P., J.A.B., J.F., and A.R.

ACKNOWLEDGMENTS

We thank Leopoldo Laricchia-Robbio and Montserrat Barragan for helpful discussions about project design. We also thank José Miguel Andrés Vaquero, Antoni Ventura, Cristina Pardo, and the personnel of the technical platforms at the CMRB for excellent technical assistance. J.P. is partially supported by the Juan de la Cierva program (MINECO). Additional support was provided by grants from the Spanish Ministry of Economy and Competitiveness MINECO (SAF2015-69706-R and SAF2015-68073-R), Instituto de Salud Carlos III-ISCIII/FEDER (Red de Terapia Celular - TerCel RD12/0019/0019 and RD12/0019/0023), AGAUR (2014-SGR-1460), and Fundació La Marató de TV3 (201534-30). J.F. is partially supported by the Ragnar Söderberg Foundation and Stiftelsen Olle Engkvist Byggmästare.

Received: February 24, 2016
Revised: June 10, 2016
Accepted: September 13, 2016
Published: October 11, 2016

REFERENCES

Batta, K., Florkowska, M., Kouskoff, V., and Lacaud, G. (2014). Direct reprogramming of murine fibroblasts to hematopoietic progenitor cells. Cell Rep. *9*, 1871–1884.

Brouwer, M., Zhou, H., and Nadif Kasri, N. (2016). Choices for Induction of Pluripotency: Recent Developments in Human Induced Pluripotent Stem Cell Reprogramming Strategies. Stem Cell Rev. *12*, 54–72.

Capellera-Garcia, S., Pulecio, J., Dhulipala, K., Siva, K., Rayon-Estrada, V., Singbrant, S., Sommarin, M.N., Walkley, C.R., Soneji, S., Karlsson, G., et al. (2016). Defining the Minimal Factors Required for Erythropoiesis through Direct Lineage Conversion. Cell Rep. *15*, 2550–2562.

Ceccaldi, R., Parmar, K., Mouly, E., Delord, M., Kim, J.M., Regairaz, M., Pla, M., Vasquez, N., Zhang, Q.S., Pondarre, C., et al. (2012). Bone marrow failure in Fanconi anemia is triggered by an exacerbated p53/p21 DNA damage response that impairs hematopoietic stem and progenitor cells. Cell Stem Cell *11*, 36–49.

Charrier, S., Ferrand, M., Zerbato, M., Précigout, G., Viornery, A., Bucher-Laurent, S., Benkhelifa-Ziyyat, S., Merten, O.W., Perea, J., and Galy, A. (2011). Quantification of lentiviral vector copy numbers in individual hematopoietic colony-forming cells shows vector dose-dependent effects on the frequency and level of transduction. Gene Ther. *18*, 479–487.

Cho, J. (2015). A paradigm shift in platelet transfusion therapy. Blood *125*, 3523–3525.

Daniel, M.G., Lemischka, I.R., and Moore, K. (2016). Converting cell fates: generating hematopoietic stem cells de novo via transcription factor reprogramming. Ann. N Y Acad. Sci. *1370*, 24–35.

Debili, N., Coulombel, L., Croisille, L., Katz, A., Guichard, J., Breton-Gorius, J., and Vainchenker, W. (1996). Characterization of a bipotent erythro-megakaryocytic progenitor in human bone marrow. Blood *88*, 1284–1296.

Doré, L.C., and Crispino, J.D. (2011). Transcription factor networks in erythroid cell and megakaryocyte development. Blood *118*, 231–239.

Dull, T., Zufferey, R., Kelly, M., Mandel, R.J., Nguyen, M., Trono, D., and Naldini, L. (1998). A third-generation lentivirus vector with a conditional packaging system. J. Virol. *72*, 8463–8471.

Ebina, W., and Rossi, D.J. (2015). Transcription factor-mediated reprogramming toward hematopoietic stem cells. EMBO J. *34*, 694–709.

Emmrich, S., Henke, K., Hegermann, J., Ochs, M., Reinhardt, D., and Klusmann, J.H. (2012). miRNAs can increase the efficiency of ex vivo platelet generation. Ann. Hematol. *91*, 1673–1684.

Feng, Q., Shabrani, N., Thon, J.N., Huo, H., Thiel, A., Machlus, K.R., Kim, K., Brooks, J., Li, F., Luo, C., et al. (2014). Scalable generation of universal platelets from human induced pluripotent stem cells. Stem Cell Reports *3*, 817–831.

Fuentes, R., Wang, Y., Hirsch, J., Wang, C., Rauova, L., Worthen, G.S., Kowalska, M.A., and Poncz, M. (2010). Infusion of mature megakaryocytes into mice yields functional platelets. J. Clin. Invest. *120*, 3917–3922.

González-Murillo, A., Lozano, M.L., Alvarez, L., Jacome, A., Almarza, E., Navarro, S., Segovia, J.C., Hanenberg, H., Guenechea, G., Bueren, J.A., and Río, P. (2010). Development of lentiviral vectors with optimized transcriptional activity for the gene therapy of patients with Fanconi anemia. Hum. Gene Ther. *21*, 623–630.

Graf, T., and Enver, T. (2009). Forcing cells to change lineages. Nature *462*, 587–594.

Guo, Y., Niu, C., Breslin, P., Tang, M., Zhang, S., Wei, W., Kini, A.R., Paner, G.P., Alkan, S., Morris, S.W., et al. (2009). c-Myc-mediated control of cell fate in megakaryocyte-erythrocyte progenitors. Blood *114*, 2097–2106.

Han, D.W., Tapia, N., Hermann, A., Hemmer, K., Höing, S., Araúzo-Bravo, M.J., Zaehres, H., Wu, G., Frank, S., Moritz, S., et al. (2012). Direct reprogramming of fibroblasts into neural stem cells by defined factors. Cell Stem Cell *10*, 465–472.

Huang, Z., Dore, L.C., Li, Z., Orkin, S.H., Feng, G., Lin, S., and Crispino, J.D. (2009). GATA-2 reinforces megakaryocyte development in the absence of GATA-1. Mol. Cell. Biol. *29*, 5168–5180.

Kuvardina, O.N., Herglotz, J., Kolodziej, S., Kohrs, N., Herkt, S., Wojcik, B., Oellerich, T., Corso, J., Behrens, K., Kumar, A., et al. (2015). RUNX1 represses the erythroid gene expression program during megakaryocytic differentiation. Blood *125*, 3570–3579.

Lalit, P.A., Salick, M.R., Nelson, D.O., Squirrell, J.M., Shafer, C.M., Patel, N.G., Saeed, I., Schmuck, E.G., Markandeya, Y.S., Wong, R., et al. (2016). Lineage reprogramming of fibroblasts into proliferative induced cardiac progenitor cells by defined factors. Cell Stem Cell *18*, 354–367.

Lecine, P., Italiano, J.E., Jr., Kim, S.W., Villeval, J.L., and Shivdasani, R.A. (2000). Hematopoietic-specific beta 1 tubulin participates in a pathway of platelet biogenesis dependent on the transcription factor NF-E2. Blood *96*, 1366–1373.

Loose, M., Swiers, G., and Patient, R. (2007). Transcriptional networks regulating hematopoietic cell fate decisions. Curr. Opin. Hematol. *14*, 307–314.

Lujan, E., Chanda, S., Ahlenius, H., Südhof, T.C., and Wernig, M. (2012). Direct conversion of mouse fibroblasts to self-renewing, tripotent neural precursor cells. Proc. Natl. Acad. Sci. USA *109*, 2527–2532.

Nakamura, S., Takayama, N., Hirata, S., Seo, H., Endo, H., Ochi, K., Fujita, K., Koike, T., Harimoto, K., Dohda, T., et al. (2014). Expandable megakaryocyte cell lines enable clinically applicable generation of platelets from human induced pluripotent stem cells. Cell Stem Cell *14*, 535–548.

Ono, Y., Wang, Y., Suzuki, H., Okamoto, S., Ikeda, Y., Murata, M., Poncz, M., and Matsubara, Y. (2012). Induction of functional platelets from mouse and human fibroblasts by p45NF-E2/Maf. Blood *120*, 3812–3821.

Orkin, S.H., and Zon, L.I. (2008). Hematopoiesis: an evolving paradigm for stem cell biology. Cell *132*, 631–644.

Pang, L., Weiss, M.J., and Poncz, M. (2005). Megakaryocyte biology and related disorders. J. Clin. Invest. *115*, 3332–3338.

Patel, S.R., Hartwig, J.H., and Italiano, J.E., Jr. (2005). The biogenesis of platelets from megakaryocyte proplatelets. J. Clin. Invest. *115*, 3348–3354.

Pawlikowska, P., Fouchet, P., Vainchenker, W., Rosselli, F., and Naim, V. (2014). Defective endomitosis during megakaryopoiesis leads to thrombocytopenia in Fanca-/- mice. Blood *124*, 3613–3623.

Pimanda, J.E., and Göttgens, B. (2010). Gene regulatory networks governing haematopoietic stem cell development and identity. Int. J. Dev. Biol. *54*, 1201–1211.

Pineault, N., Robert, A., Cortin, V., and Boyer, L. (2013). Ex vivo differentiation of cord blood stem cells into megakaryocytes and platelets. Methods Mol. Biol. *946*, 205–224.

Pulecio, J., Nivet, E., Sancho-Martinez, I., Vitaloni, M., Guenechea, G., Xia, Y., Kurian, L., Dubova, I., Bueren, J., Laricchia-Robbio, L., and Izpisua Belmonte, J.C. (2014). Conversion of human fibroblasts into monocyte-like progenitor cells. Stem Cells *32*, 2923–2938.

Riddell, J., Gazit, R., Garrison, B.S., Guo, G., Saadatpour, A., Mandal, P.K., Ebina, W., Volchkov, P., Yuan, G.C., Orkin, S., et al. (2014). Reprogramming committed murine blood cells to induced hematopoietic stem cells with defined factors. Cell *157*, 549–564.

Ring, K.L., Tong, L.M., Balestra, M.E., Javier, R., Andrews-Zwilling, Y., Li, G., Walker, D., Zhang, W.R., Kreitzer, A.C., and Huang, Y. (2012). Direct reprogramming of mouse and human fibroblasts into multipotent neural stem cells with a single factor. Cell Stem Cell *11*, 100–109.

Río, P., Segovia, J.C., Hanenberg, H., Casado, J.A., Martínez, J., Göttsche, K., Cheng, N.C., Van de Vrugt, H.J., Arwert, F., Joenje, H., and Bueren, J.A. (2002). In vitro phenotypic correction of hematopoietic progenitors from Fanconi anemia group A knockout mice. Blood *100*, 2032–2039.

Robb, L., Elwood, N.J., Elefanty, A.G., Köntgen, F., Li, R., Barnett, L.D., and Begley, C.G. (1996). The scl gene product is required for the generation of all hematopoietic lineages in the adult mouse. EMBO J. *15*, 4123–4129.

Schlaeger, T.M., Daheron, L., Brickler, T.R., Entwisle, S., Chan, K., Cianci, A., DeVine, A., Ettenger, A., Fitzgerald, K., Godfrey, M., et al. (2015). A comparison of non-integrating reprogramming methods. Nat. Biotechnol. *33*, 58–63.

Shivdasani, R.A., Rosenblatt, M.F., Zucker-Franklin, D., Jackson, C.W., Hunt, P., Saris, C.J., and Orkin, S.H. (1995). Transcription factor NF-E2 is required for platelet formation independent of the actions of thrombopoietin/MGDF in megakaryocyte development. Cell *81*, 695–704.

Sim, X., Poncz, M., Gadue, P., and French, D.L. (2016). Understanding platelet generation from megakaryocytes: implications for in vitro-derived platelets. Blood *127*, 1227–1233.

Sykes, S.M., and Scadden, D.T. (2013). Modeling human hematopoietic stem cell biology in the mouse. Semin. Hematol. *50*, 92–100.

Szabo, E., Rampalli, S., Risueño, R.M., Schnerch, A., Mitchell, R., Fiebig-Comyn, A., Levadoux-Martin, M., and Bhatia, M. (2010). Direct conversion of human fibroblasts to multilineage blood progenitors. Nature *468*, 521–526.

Tijssen, M.R., Cvejic, A., Joshi, A., Hannah, R.L., Ferreira, R., Forrai, A., Bellissimo, D.C., Oram, S.H., Smethurst, P.A., Wilson, N.K., et al. (2011). Genome-wide analysis of simultaneous GATA1/2, RUNX1, FLI1, and SCL binding in megakaryocytes identifies hematopoietic regulators. Dev. Cell *20*, 597–609.

Tsai, F.Y., Keller, G., Kuo, F.C., Weiss, M., Chen, J., Rosenblatt, M., Alt, F.W., and Orkin, S.H. (1994). An early haematopoietic defect in mice lacking the transcription factor GATA-2. Nature *371*, 221–226.

Vierbuchen, T., and Wernig, M. (2011). Direct lineage conversions: unnatural but useful? Nat. Biotechnol. *29*, 892–907.

Wang, D., Villasante, A., Lewis, S.A., and Cowan, N.J. (1986). The mammalian beta-tubulin repertoire: hematopoietic expression of a novel, heterologous beta-tubulin isotype. J. Cell Biol. *103*, 1903–1910.

Wang, Y., Hayes, V., Jarocha, D., Sim, X., Harper, D.C., Fuentes, R., Sullivan, S.K., Gadue, P., Chou, S.T., Torok-Storb, B.J., et al. (2015). Comparative analysis of human ex vivo-generated platelets vs megakaryocyte-generated platelets in mice: a cautionary tale. Blood *125*, 3627–3636.

Xu, J., Du, Y., and Deng, H. (2015). Direct lineage reprogramming: strategies, mechanisms, and applications. Cell Stem Cell *16*, 119–134.

Yu, B., He, Z.Y., You, P., Han, Q.W., Xiang, D., Chen, F., Wang, M.J., Liu, C.C., Lin, X.W., Borjigin, U., et al. (2013). Reprogramming fibroblasts into bipotential hepatic stem cells by defined factors. Cell Stem Cell *13*, 328–340.